Consiglio Nazionale delle Ricerche

THE EFFECTS OF SPACECRAFT AND UPPER STAGE BREAKUPS ON THE GEOSTATIONARY RING

Luciano Anselmo, Carmen Pardini

Rapporto CNUCE-B4-2000-002

CNUCE

Pisa

THE EFFECTS OF SPACECRAFT AND UPPER STAGE BREAKUPS ON THE GEOSTATIONARY RING

Report CNUCE-B4-2000-002
January 12, 2000

Luciano Anselmo
Carmen Pardini

Consiglio Nazionale delle Ricerche
Istituto CNUCE, Via S. Maria 36, PISA

Abstract

The environmental effects of spacecraft and rocket body breakups affecting the geostationary ring were analyzed with a novel approach. Six explosions were simulated: one in geostationary orbit, two in near-synchronous orbit and three in geostationary transfer orbit. The debris clouds were propagated for 10 years, taking into account all the relevant perturbations, and the resulting contribution to the object density in the geostationary ring was computed numerically as a function of debris size and time.

On the short term, the explosions in geostationary orbit are the most detrimental for the environment, producing for several months density peaks higher or comparable to the background in the overall size range. However, the natural perturbations mitigate considerably the problem after one year, although a few tens of complete breakups could produce a long-term average density matching the existing debris background.

High intensity explosions in near-synchronous orbit may significantly affect the environment, both short and long term, by generating a large number of millimeter sized particles crossing the geostationary ring. Again, a few tens of complete breakups might produce long term effects comparable to the existing background, but the peak density of the objects larger than 1 cm would remain much lower.

The explosions in geostationary transfer orbit, on the other hand, do not contribute significantly to the object density in the geostationary ring. Only a fragmentation at one of the first apogees may produce a sharp local density peak above the background, but a few months of orbital perturbations are sufficient to reduce dramatically that contribution. Hundreds of breakups in transfer orbit would be needed to obtain an object density in the geostationary ring comparable to the background.

Although some care is needed to translate from object densities into collision rates, the results presented strongly support the generalized re-orbiting of geostationary spacecraft at the end of their operational life.

Introduction

Since the seminal proposal by A. C. Clarke in 1945 [1], the geostationary orbit (GEO) was regarded as a resource of great future potential, offered by the laws of celestial mechanics to humankind. Such a promise began to materialize in the 1960s, after the launch of the first geosynchronous communication spacecraft, and in the following decades there was a rapid growth in the number of satellites operated in the GEO regime. In total, about 600 geosynchronous satellites and 200 apogee rocket stages have been launched since Syncom 1, in 1963.

In the 1980s, the very rapid increase of spacecraft in GEO and the growing role of private operators in the field rose the concern of a possible overcrowding of the geostationary ring, jeopardizing in the long-term the exploitation of such irreplaceable space resource. Several authors concentrated their analysis on the long-term evolution of abandoned satellites and, in a few cases, the risk of collision between space objects in GEO was estimated [2–5], in particular to devise affordable and effective end-of-life disposal measures [6].

During the 1990s, it became clear that also spacecraft and upper stage breakups contributed to the GEO debris environment. T. Yasaka and its group, in Japan, carried out extensive investigations

of the global GEO debris environment long-term evolution, based on a simple object accumulation model [7–12], while other authors [13] studied the short-term collision risk represented by explosions affecting the geostationary ring.

The aim of the work presented in this paper was to try to close the gap between short and long-term analysis. A new modeling approach and specific software tools were developed to provide a high fidelity description of a debris cloud evolution and its interaction with the spacecraft in the geostationary ring. Six typical explosions, affecting the GEO regime and belonging to breakup categories already observed in practice, were simulated and accurately propagated for 10 years, including all the relevant perturbations. For each fragmentation, the additional contribution to the object density in GEO was computed as a function of time, debris size and right ascension (i.e. position along the ring). These results were therefore compared with the debris background, in order to assess the additional collision risk entailed by each specific fragmentation event.

Simulated Fragmentation Events

Six fragmentation events affecting the GEO regime were simulated: a spacecraft low intensity explosion in the geostationary ring, two Titan Transtage high intensity explosions in near-synchronous orbit (at the ascending node and at the maximum declination) and three Ariane IV third stage low intensity explosions in geostationary transfer orbit (GTO). For the last three explosions, in order to investigate the impact of the orbital perturbations on the parent object orbit, one simulation was carried at the first apogee and the others at the perigee and apogee of a 4.5 months old GTO.

These explosions represent classes of events already recorded in space [14]. The parameters adopted for the simulations are listed in Table 1, while in Table 2 the osculating – true of date – elements of the parent objects at the simulated explosion epochs are given.

TABLE 1. SIMULATED FRAGMENTATION EVENTS

Simulation Number	Parent Object Class	Parent Object Mass (kg)	Explosion Class	Breakup Altitude (km)	Breakup Right Ascension (deg)	Breakup Declination (deg)
1	Satellite in the GEO Ring	2000	Low Intensity	35789	298	0
2	Near-Synchronous Titan Transtage	2555	High Intensity	38620	34	0
3	Near-Synchronous Titan Transtage	2555	High Intensity	37304	124	14
4	Ariane IV 3rd Stage in GTO	1760	Low Intensity	35786	83	0
5	Ariane IV 3rd Stage in 4.5 mo. old GTO	1760	Low Intensity	269	162	- 6
6	Ariane IV 3rd Stage in 4.5 mo. old GTO	1760	Low Intensity	35088	340	6

TABLE 2. ORBITAL ELEMENTS OF PARENT OBJECTS AT FRAGMENTATION

Simulation Number	Explosion Epoch (yyyy-mm-dd hh:mm:ss.ss)	Semimajor Axis (km)	Eccentricity	Inclination (deg)	Right Ascension of Node (deg)	Argument of Perigee (deg)	Mean Anomaly (deg)
1	1999-05-11 03:32:29.57	42164.55	0.00007474	0.1082	74.7137	64.4827	158.7451
2	1999-05-16 07:33:31.16	43614.40	0.031842	13.9430	33.6380	184.6000	175.0940
3	1999-05-16 14:07:31.16	43614.20	0.031870	13.9430	33.6360	184.5510	269.0340
4	2000-05-07 15:00:00.00	24371.14	0.7301	7.0000	83.0000	180.0000	180.0000
5	1999-05-07 13:50:42.91	24054.75	0.72368864	7.0724	222.3311	297.5088	0.1708
6	1999-05-07 08:41:12.91	24056.35	0.72369921	7.0721	222.4219	297.3304	180.0978

The breakups were modeled using the CLDSIM software developed at CNUCE [15–17], while the resulting debris clouds were propagated for a 10-year time interval with a modified, multi-object version of the ASAP numerical integrator developed at JPL [18]. The perturbations included were the geopotential (8 x 8 gravity field), the luni-solar attraction and the radiation pressure with eclipses. For the three events in GTO, the atmospheric drag was included as well.

To represent the fragment mass distribution for low intensity explosions (spacecraft in the GEO ring and Ariane IV third stage), the following classical relationship was adopted [19]:

$$N(m) = \begin{cases} 0.171M\ e^{-0.6502\sqrt{m}} & m \geq 1.936 \\ 0.869M\ e^{-1.8202\sqrt{m}} & m < 1.936 \end{cases} \tag{1}$$

where M (kg) is the exploding mass and N is the cumulative number of fragments with a mass larger than m (kg). For high intensity explosions (Titan Transtage), 90% of the exploding mass follows an exponential distribution law, while 10% follow a power law. The requirements of mass conservation and function continuity set the value of the numerical coefficients N_0 and c [20]:

$$N(m) = \begin{cases} N_0 e^{-c\sqrt{m}} & m \geq 0.05 \\ 0.439\left(\dfrac{m}{0.1 \cdot M}\right)^{-0.75} & m < 0.05 \end{cases} \tag{2}$$

The mass m (kg) and the cross-sectional area A (m^2) of the debris generated were related through the following relationship [21]:

$$m = \begin{cases} 62.013A^{1.13} & A \geq 8.04 \cdot 10^{-5} \\ 2030.33A^{1.5} & A < 8.04 \cdot 10^{-5} \end{cases} \tag{3}$$

The mass of each fragment was used to compute a corresponding average cross-section by inverting equation (3); the actual area was then randomly extracted from an appropriate log-normal distribution [20]. The debris diameters were obtained assuming a spherical shape.

To find the orbits of the breakup fragments, the classical velocity distribution given in [21] was adopted:

$$\log(\overline{\Delta V}) = -0.0676(\log d)^2 - 0.804 \log d - 1.514 \tag{4}$$

where $\overline{\Delta V}$ (km/s) is the average ejection velocity and d (m) is the fragment diameter. The actual velocity increment of each fragment (ΔV) was obtained from the triangular distribution [22]:

$$\Delta V = \begin{cases} \overline{\Delta V}\left(0.1 + 0.6\sqrt{3y}\right) & 0.00 \le y < 0.75 \\ \overline{\Delta V}\left(1.3 - 0.6\sqrt{1-y}\right) & 0.75 \le y \le 1.00 \end{cases} \tag{5}$$

where y is a random number between 0 and 1. Because the breakup events were assumed isotropic, the velocity vector of each piece of debris was obtained by adding to the velocity of the parent object a vector of magnitude ΔV and random direction.

All the fragments with mass ≥ 10 g were propagated, but the smaller objects, due to their large number (especially for high intensity explosions), were sampled and only the representative particles were propagated, with the implicit assumption that the orbital evolution of the debris represented by them would be the same. The sampling factors used – as a function of the debris mass m (kg) – were:

- 1% for $10^{-6} \le m < 10^{-5}$;
- 10% for $10^{-5} \le m < 10^{-4}$;
- 20% for $10^{-4} \le m < 10^{-2}$;
- 100% for $m \ge 10^{-2}$.

Table 3 summarizes the number of debris – of diameter d – produced by each simulated explosion, and the corresponding number of sampled particles propagated for 10 years. In total, more than 830,000 fragments of mass ≥ 1 mg were simulated and about 36,000 were propagated.

TABLE 3. NUMBER OF DEBRIS PRODUCED AND SAMPLED FOR PROPAGATION

Simulation Number	1 mm ≤ *d* < 1 cm		1 cm ≤ *d* < 10 cm		10 cm ≤ *d* < 1 m		1 m ≤ *d* < 10 m	
	Produced	Sampled	Produced	Sampled	Produced	Sampled	Produced	Sampled
1	85	15	937	793	672	672	17	17
2	364,220	14,262	3,532	1,224	210	210	28	28
3	371,480	14,295	3,497	1,217	210	210	28	28
4	65	11	455	387	332	332	9	9
5	40	8	827	707	581	581	14	14
6	15	3	460	392	358	358	14	14

Debris Density Computations

The aim of the research presented in this paper was to assess the contribution of occasional explosions to the object density in the GEO ring, where most of the active synchronous satellites spend their operational life. For the purposes of the present study, the GEO ring was defined as the volume of space centered on the geostationary orbit (mean altitude of 35,786 km, zero inclination), ± 75 km in altitude and ± 0.1° in declination (geocentric latitude).

The object density in the GEO ring was obtained in the following way:

1. The GEO ring was subdivided in right ascension sectors, or cells, of assigned amplitude (for instance 5°, as in the histograms presented later in this paper);
2. At any given epoch after the simulated explosion (for instance after 2 days, 6 months, or 10 years), the mean anomaly intervals ΔM, corresponding to the orbital crossings of the right ascension cells in the GEO ring, were numerically computed for each representative debris produced by the simulated explosions;
3. Taking into account the i^{th} debris diameter d, sampling factor s_i and fractional contribution per orbit $\Delta M_{ij}/2\pi$, it was then easy to compute the average object density ρ_j for the j^{th} right ascension cell:

$$\rho_j(d) = \frac{\sum_i^N s_i(d) \frac{\Delta M_{ij}}{2\pi}}{V_j} \tag{6}$$

with the cell volume V_j given by:

$$V_j = \left(2\, R_0^{\,2} + \frac{1}{6} \Delta R^2 \right) \sin\frac{\Delta\delta}{2} \Delta R\, \Delta\alpha \tag{7}$$

where R_0 is the geostationary orbit mean radius vector, and ΔR, $\Delta\delta$ and $\Delta\alpha$ define the cell size in altitude, declination and right ascension, respectively.

Simulation Results

The debris particles – with mass ≥ 1 mg – produced by the simulated explosions were propagated, taking into account all the relevant perturbations, for 10 years, saving the results at intermediate times (typically every two months). Any saved file provided a snapshot of the debris orbital spreading at a particular explosion elapsed time. By using the mathematical approach described in the previous section, it was then possible to translate from orbital distribution into debris density in the GEO ring, making possible a comparison with the actual background environment, for a relative collision risk evaluation as a function of the explosion class and elapsed time.

The amount of data obtained was cumbersome, and only some general results can be summarized and discussed in a paper of reasonable length. However, it must be stressed that the details may be very important to fully understand particular situations and that the analysis technique presented here can provide the high definition results needed in such cases.

The background debris density in the GEO ring, to be compared with the results of the simulations, is shown in Figure 1. It was obtained, by the method described in the previous section, from the CNUCE orbital debris reference model [17], based on the simulation of past fragmentation events and updated to January 1, 1999. The average background density found was 3.76×10^{-8} km^{-3} for debris larger than 1 mm, 3.50×10^{-8} km^{-3} for debris larger than 1 cm, and 3.47×10^{-8} km^{-3} for debris larger than 10 cm. However, these values must be considered a lower limit, because the knowledge of the environment at GEO altitude is still quite incomplete, even for large objects [23].

Case 1: Satellite in the GEO Ring

The low intensity explosion of an operational geostationary satellite produces a sizable amount of debris affecting the GEO ring. However, as shown in Figures 2-4, the orbital plane evolution, due mainly to the luni-solar perturbations, reduces significantly, in a few years, the intervals of right ascension crossed by the fragments. But the debris orbital inclinations come back close to zero about 54 years after the explosion, even though the orbital perturbations, including the solar radiation pressure, have enough time to increase the eccentricities and spread the nodes, relieving the burden on the GEO ring.

The density histograms shown in Figures 5-8 confirm the qualitative impression given by Figures 2-4. Due to the nature of the simulated explosion, there is a small number of millimetric particles and a comparable number of centimetric and metric fragments (see Table 3).

Immediately after the explosion (Figure 5), occurring at 298° of right ascension, nearly all the GEO ring is affected by a debris density increase, with a clear maximum around the breakup point. There, the fragment density exceeds the artificial debris background by a factor 3–6, depending on the size. But after one year (Figure 6), the density peak is already reduced by a factor 20, well below the background density, while several holes begin to appear in the right ascension distribution, in particular for objects larger than 10 cm. This trend is confirmed after 5 (Figure 7) and 10 years (Figure 8), when the debris density contribution to the GEO ring is concentrated in two right ascensions intervals, approximately 180° apart, with maximum values at least 30 times lower than the background.

A longer term analysis was outside the scope of the study presented in this paper. However, when the orbital inclinations of most fragments come back close to zero, about 54 years after the explosion, the combined effects of geopotential harmonics, luni-solar attraction and solar radiation pressure result in an object density in the GEO ring quite lower than the background.

Cases 2 and 3: Titan Transtage in Near-Synchronous Orbit

The high intensity explosion of an abandoned Titan Transtage in near-synchronous orbit (see Tables 1–3) presents many interesting features.

Figures 9–12 show the results for Case 2, where a breakup at the ascending node, 2834 km above the GEO average altitude, was simulated. Soon after the explosion (Figure 9), due to the orbital geometry, fragments larger than 1 cm cross the GEO ring only about 180° apart from the breakup right ascension, with an object density more than 30 times lower than the background. On the other hand, many millimetric particles, typically ejected at higher speeds, cross most of the GEO ring. A maximum is found around (but not exactly at – for obvious dynamical reasons) the breakup right ascension, and 180° apart: the local fragment densities are comparable to the artificial debris background.

One year after the explosion (Figure 10), the density of millimetric particles decreases below the background, while the contribution of the fragments larger than 1 cm becomes two orders of magnitude lower. After 5 (Figure 11) and 10 years (Figure 12), a further spreading in right ascension is observed, but the local fragment densities remain low with respect to the background, by an order of magnitude if larger than 1 mm, and by two orders of magnitude if larger than 1 cm.

Figures 13–15 shows the evolution, in terms of right ascension and declination, of the debris produced by a Transtage high intensity explosion at the maximum declination of its orbit (Case 3, see Tables 1–3). Several years are needed to obtain a nearly uniform distribution of the nodes.

Again, the density histograms confirm this qualitative picture. Soon after the explosion (Figures 13 and 16), the two forbidden gaps along the GEO ring are evident. One of them, as the narrow equivalent of Case 2 (see Figure 9), lies around the breakup right ascension, while the other is about 180° apart. The maximum local density of millimetric particles is four times lower than the background, while for the fragments larger than 1 cm, whose maximum concentration is found around the nodes of the Transtage original orbit, the density is two orders of magnitude less.

After one year (Figure 17), the distribution pattern and densities are practically the same; only after several years (Figures 18 and 19) a broader distribution in right ascension prevails, with approximately stable peak density values (the detailed behavior depends on the debris size).

Cases 4, 5 and 6: Ariane IV Third Stage in GTO

Three Ariane IV third stage low intensity explosions in GTO were simulated: at the first apogee (Case 4), and both at the perigee (Case 5) and the apogee (Case 6) of a 4.5 months old orbit (see Tables 1-3). In all cases, the number of millimetric particles generated was a small fraction of the total.

In Case 4, immediately after the explosion, there is only a sharp density peak around the breakup right ascension (83°). There, the density contribution to the GEO ring is 1×10^{-7} km^{-3} for

fragments larger than 1 cm (3 times the background), and less than 3×10^{-8} km^{-3} for those larger than 10 cm (approximately equivalent to the background). After one year, the resulting debris cloud crosses about 60° of the GEO ring, but with a peak density contribution reduced by more than two orders of magnitude. After 10 years (Figure 21), the entire GEO ring may be interested, but the average object density is very low.

The explosion at the perigee of the old GTO (Case 5) does not produce any effect on the GEO ring, either short or long-term, because most of the fragments reenter in the Earth's atmosphere after a few hours. Even the explosion at the apogee of the old GTO (Case 6) does not produce any effect on the short-term, but after several years (Figure 22), due to orbital perturbations, some fragments begin to intersect the GEO ring, giving a contribution similar, in density and distribution, to Case 4 after about 5 years (Figure 20). In other words, the contribution to the GEO ring object density, if any, is two orders of magnitude lower than the artificial debris background.

Conclusions

The effects of spacecraft and upper stage breakups, in terms of additional contribution to the object density in the GEO ring, were analyzed with a novel approach. Six explosions were simulated - one in geostationary orbit, two in near-synchronous orbit, three in geostationary transfer orbit - and the resulting debris clouds were propagated for 10 years, taking into account all the relevant perturbations.

On the short term, the explosions in geostationary orbit (Case 1) are the most detrimental for the GEO ring environment, producing for several months density peaks higher or comparable to the background. However, the natural perturbations mitigate considerably the problem after one year, even though a few tens of complete breakups could produce long-term effects matching the existing debris background, accumulated after 600 launches and three known explosions in the synchronous regime.

High intensity explosions in near-synchronous orbit (Cases 2 and 3) may significantly affect the environment, both short and long-term, by generating a large number of millimeter sized particles crossing the GEO ring. Again, a few tens of complete breakups could produce long-term effects comparable to the existing debris background, but the peak density of the objects larger than 1 cm would remain much lower.

On the other hand, the explosions in geostationary transfer orbit do not contribute significantly to the object density in the GEO ring. Only a fragmentation at one of the first apogees may produce a sharp local density peak above the background, but a few months are sufficient to reduce dramatically that contribution. For this reason, hundreds of breakups in GTO would be needed to materialize an object density in GEO comparable to the background.

Although some care is needed to translate from object density into collision rate (the debris relative velocities must be estimated), the results presented in this paper strongly support the recommendation formulated by the Inter-Agency Space Debris Coordination Committee (IADC)

for the end-of-life re-orbiting of the geostationary spacecraft [6]. The GEO ring is an extraordinary and irreplaceable resource, which deserves any reasonable preservation effort.

Acknowledgments

The authors contributed to this paper in the framework of the Cooperation Agreement (1997-2001) between the CNUCE Institute of the National Research Council (CNR) and the Italian Space Agency (ASI).

References

[1] CLARKE, A.C. "Extra-Terrestrial Relays – Can Rocket Stations Give World-Wide Radio Coverage?", *Wireless World,* October 1945, pp. 305-308.

[2] HECHLER, M. and VAN DER HA, J.C. "The Probability of Collisions on the Geostationary Ring", *ESA Journal,* Vol. 4, No. 3, 1980, pp. XX-XX.

[3] FUSCO, G., and BURATTI, A. "Crowding of the Geostationary Orbit", Final Report, ESA Contract No. 5705/83/NL/PP (SC), RIPTO, Turin, Italy, October 1984.

[4] CHOBOTOV, V.A. "Disposal of Spacecraft at End-of-Life in Geosynchronous Orbit", in *Astrodynamics 1989*, AAS Advances in the Astronautical Sciences, Vol. 71, Univelt Inc., San Diego, California, USA, 1990, pp. 377-391.

[5] CHOBOTOV, V.A. (editor) *Orbital Mechanics*, AIAA Education Series, American Institute of Aeronautics and Astronautics, Washington, D.C., USA, 1991, Chapter 13, pp. 335-362.

[6] JOHNSON, N. "Protecting the GEO Environment: Policies and Practices", *Space Policy*, in press, 1999.

[7] YASAKA, T., and ODA, S. "Classification of Debris Orbits with Regard to Collision Hazard in Geostationary Region", paper IAA-90-571, *41st International Astronautical Congress*, Dresden, Democratic Republic of Germany, October 1990.

[8] YASAKA, T., and ISHII, N. "Breakup in Geostationary Orbit: A Possible Creation of a Debris Ring", *Acta Astronautica*, Vol. 26, No. 7, 1992, pp. 523-530.

[9] YASAKA, T., and ODA, S. "Breakup, Collision and Population Growth in Geostationary Orbit", *Proceedings of the First European Conference on Space Debris*, ESA/ESOC, Darmstadt, Germany, ESA SD-01, July 1993, pp. 645-649.

[10] YASAKA, T. "Remarks on Orbital Environment Protection at Geostationary Altitude: Results from Long Term Breakup Simulation", *Acta Astronautica*, Vol. 34, 1994, pp. 33-41.

[11] YASAKA, T., HANADA, T., and MATSUOKA, T. "Model of the Geosynchronous Debris Environment", paper IAA-96-IAA.6.3.08, *47th International Astronautical Congress*, Beijing, China, October 1996.

[12] YASAKA, T., HANADA, T., and HIRAYAMA, H. "GEO Debris Environment: A Model to Forecast the Next 100 Years", *Advances in Space Research*, Vol. 23, No. 1, 1999, pp.191-199.

[13] KAMPRATH, M.F. and JENKIN, A.B. "Debris Collision Hazard from Breakups in the Geosynchronous Ring", Submitted to *Space Debris*, 1998.

[14] JOHNSON, N. L., BADE, A., EICHLER, P., CIZEK, E., ROBERTSON, S. and SETTECERRI, T., "History of On-Orbit Satellite Fragmentations", Eleventh Edition, JSC-28383, Johnson Space Center, NASA, Houston, Texas, USA, July 31, 1998.

[15] PARDINI, C. "Development of a Single Fragmentation Event Simulator (CLDSIM)", Study Note of Work Package 3600, Study on Long Term Evolution of Earth Orbiting Debris, ESA/ESOC Contract No. 10034/92/D/IM(SC), Consorzio Pisa Ricerche, Pisa, Italy, September 1995.

[16] PARDINI, C., CORDELLI, A., ROSSI, A., ANSELMO, L. and FARINELLA, P. "The Contribution of Past Fragmentation Events to the Uncatalogued Orbital Debris Population", in *Astrodynamics 1995*, AAS Advances in the Astronautical Sciences, Vol. 90, Univelt Inc., San Diego, California, USA, 1996, pp. 809-828.

[17] PARDINI, C., ANSELMO, L., ROSSI, A., CORDELLI, A. and FARINELLA, P. "A New Orbital Debris Reference Model", *The Journal of the Astronautical Sciences,* Vol. 46, No. 3, 1998, pp. 249-265.

[18] KWOK, J. H. "The Artificial Satellite Analysis Program (ASAP)", Version 2.0, JPL NPO-17522, Pasadena, California, USA, 1987.

[19] SU, S. Y. and KESSLER, D. J. "Contribution of Explosion and Future Collision Fragments to the Orbital Debris Environment", *Advances in Space Research*, Vol. 5, No. 2, 1985, pp. 25-34.

[20] ANSELMO, L., CORDELLI, A., FARINELLA, P., PARDINI, C. and ROSSI, A. "Study on Long Term Evolution of Earth Orbiting Debris", Final Report, ESA/ESOC Contract No. 10034/92/D/IM(SC), Consorzio Pisa Ricerche, Pisa, Italy, April 1996.

[21] REYNOLDS, R. C. "Review of Current Activities to Model and Measure the Orbital Debris Environment in Low-Earth-Orbit", *Advances in Space Research*, Vol. 10, No. 3 – 4, 1990, pp. 359-372.

[22] JEHN, R. "Modelling Debris Clouds", Shaker Verlag, Aachen, Germany, 1996.

[23] TALENT, D.L., POTTER, A.E., and HENIZE, K.G. "A Search for Debris in GEO", *Proceedings of the Second European Conference on Space Debris*, ESA/ESOC, Darmstadt, Germany, ESA SP-393, May 1997, pp. 279-284.

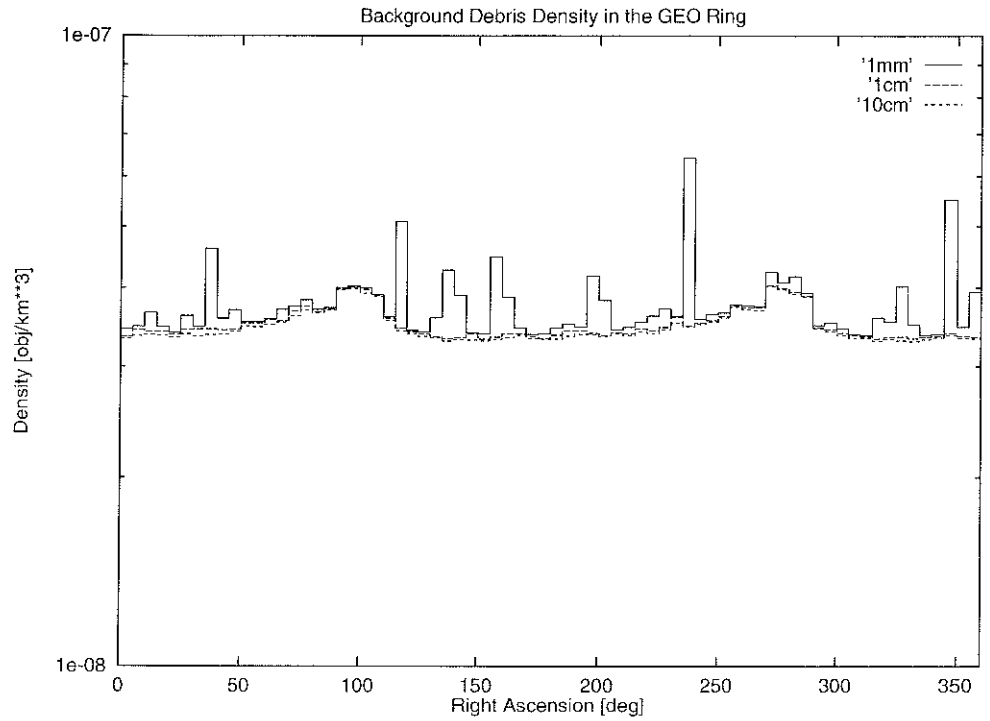

Fig. 1. Background debris density in the GEO ring for particles larger than 1 mm, 1 cm and 10 cm.

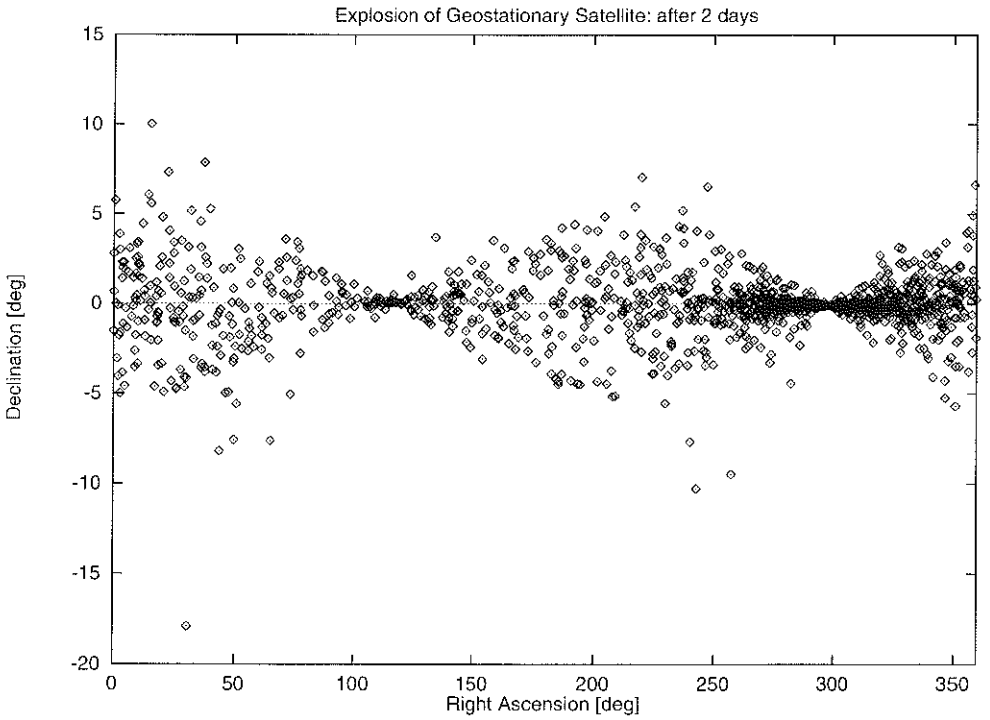

Fig. 2. Explosion in geostationary orbit: distribution of the fragments, in right ascension and declination, after 2 days.

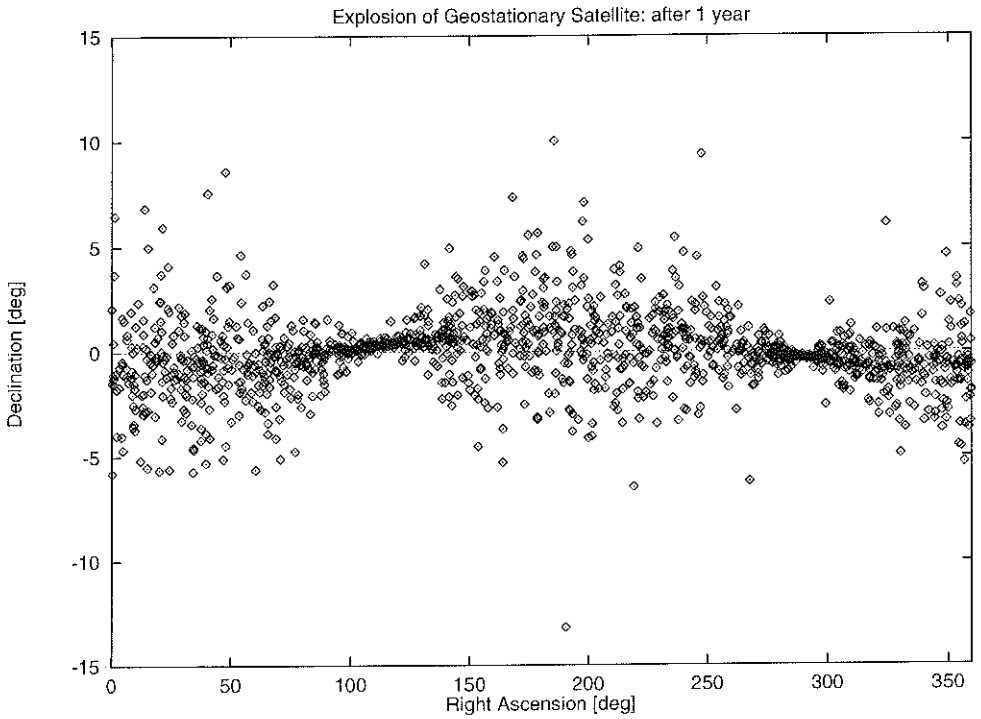

Fig. 3. Explosion in geostationary orbit: distribution of the fragments, in right ascension and declination, after 1 year.

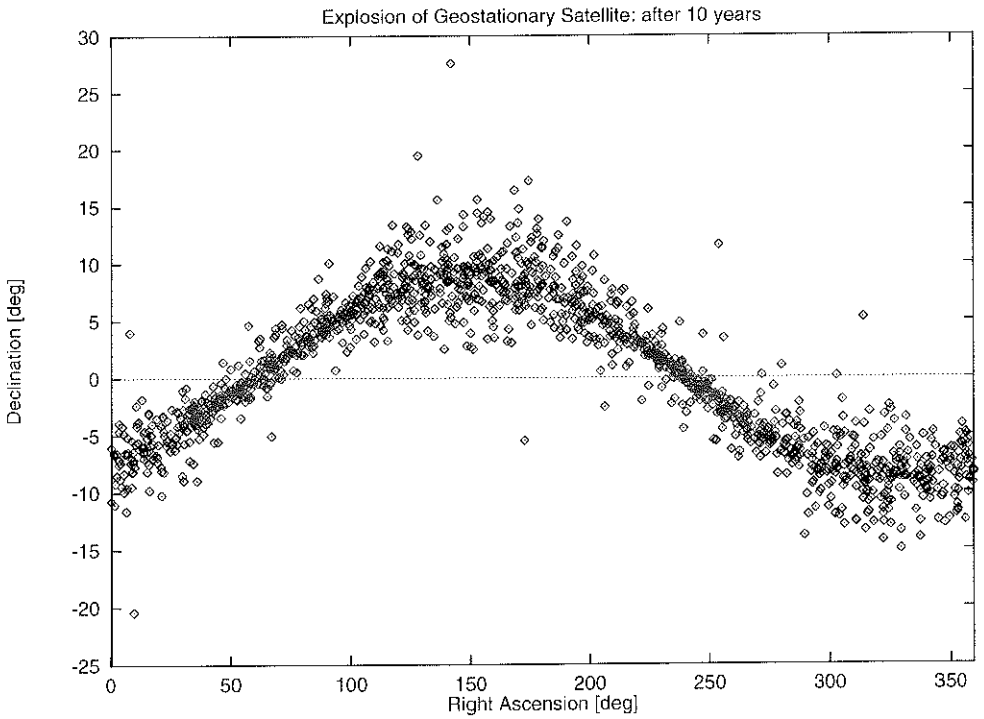

Fig. 4. Explosion in geostationary orbit: distribution of the fragments, in right ascension and declination, after 10 years.

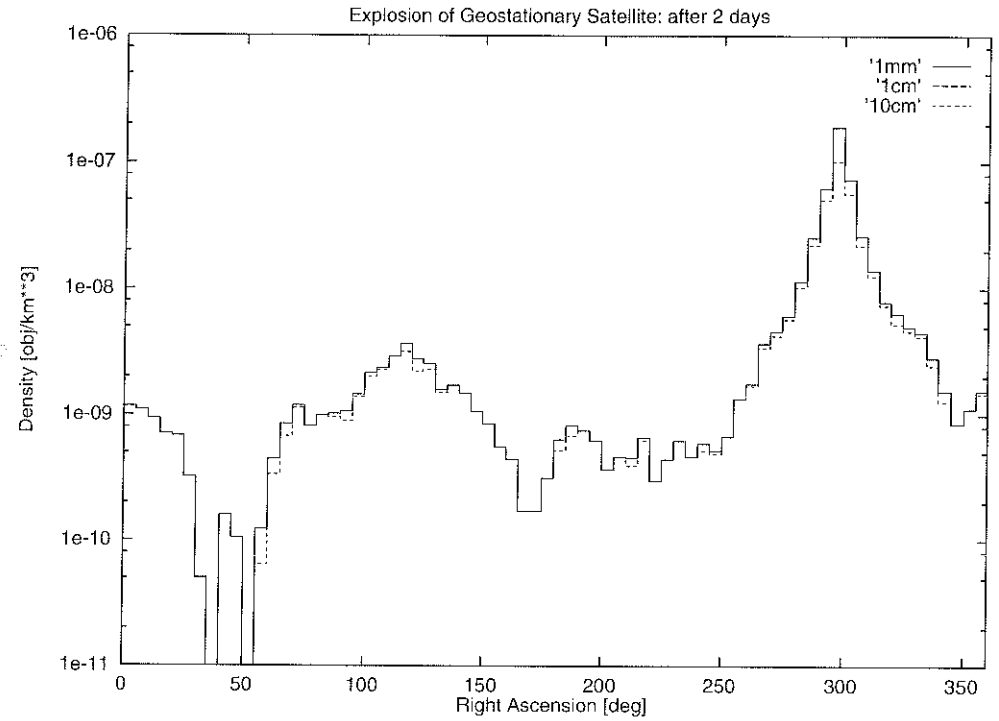

Fig. 5. Explosion in geostationary orbit: density distribution in the GEO ring after 2 days, for fragments larger than 1 mm, 1cm and10 cm.

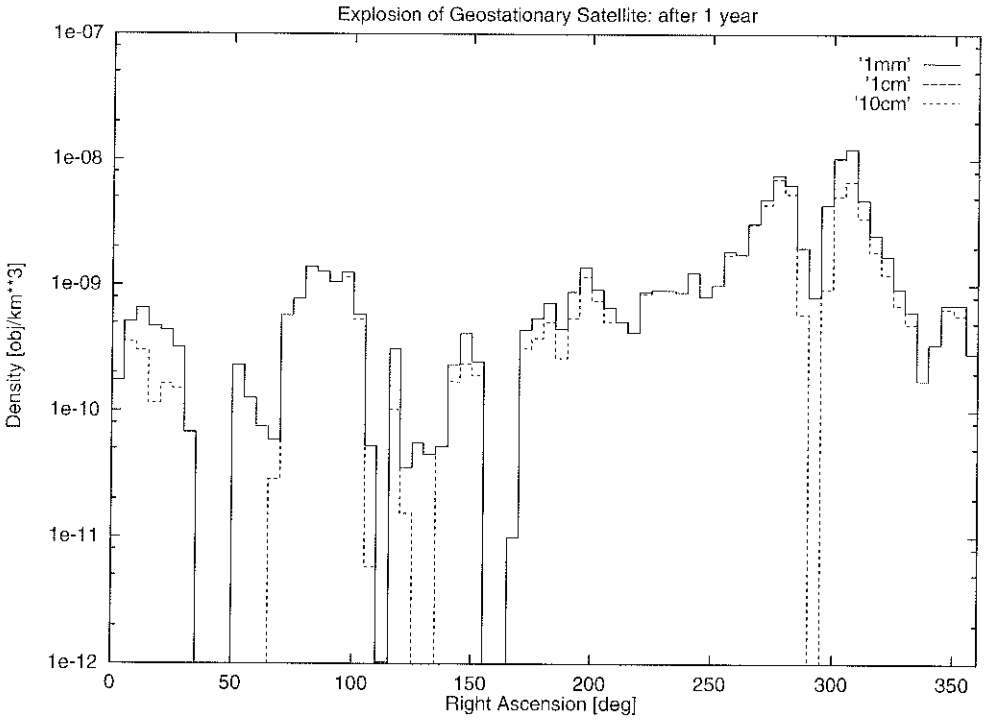

Fig. 6. Explosion in geostationary orbit: density distribution in the GEO ring after 1 year, for fragments larger than 1 mm, 1cm and 10 cm.

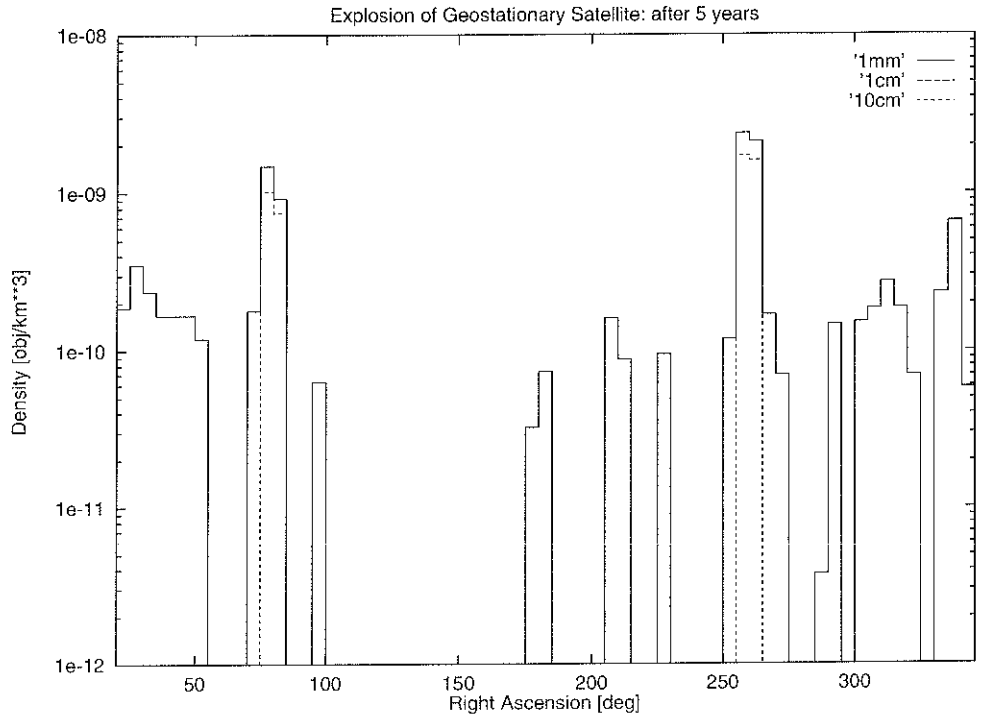

Fig. 7. Explosion in geostationary orbit: density distribution in the GEO ring after 5 years, for fragments larger than 1 mm, 1cm and 10 cm.

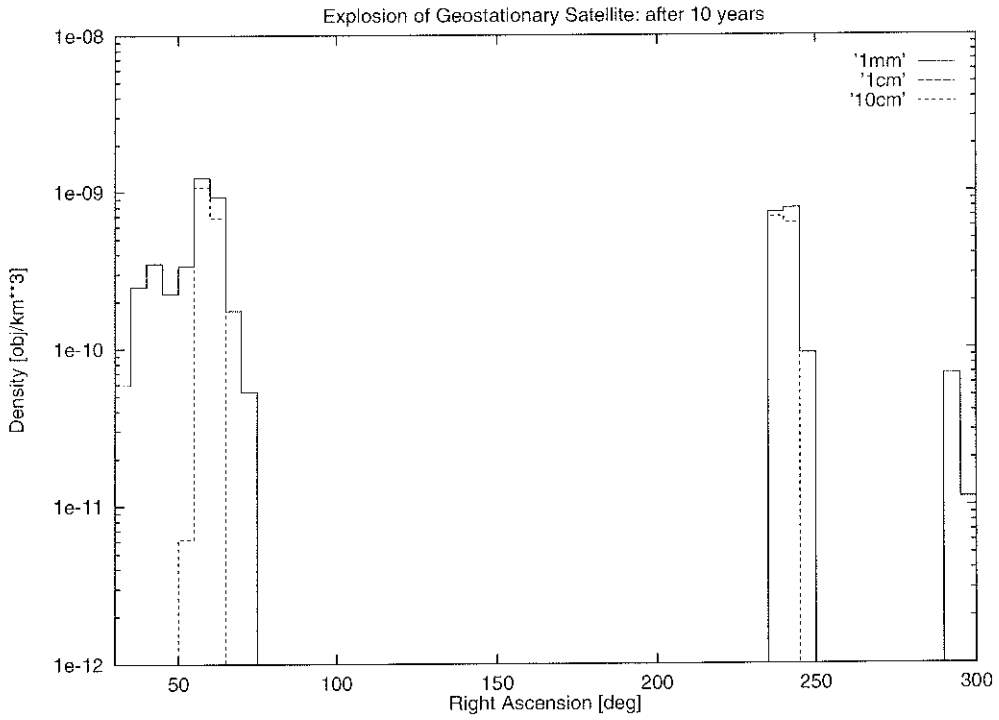

Fig. 8. Explosion in geostationary orbit: density distribution in the GEO ring after 10 years, for fragments larger than 1 mm, 1cm and 10 cm.

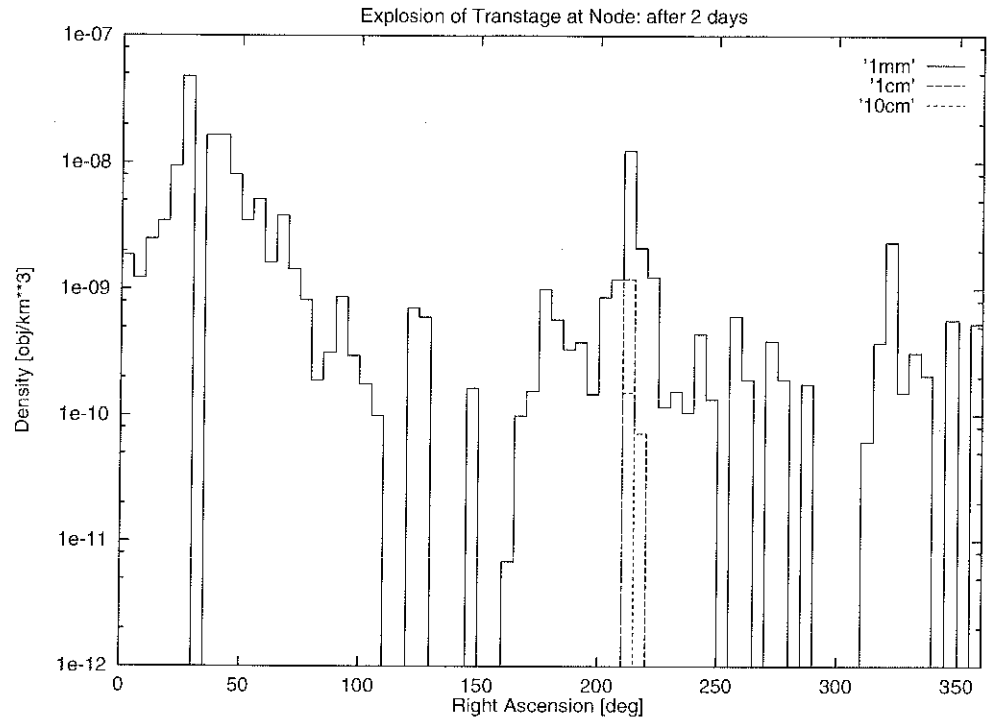

Fig. 9. Explosion at the ascending node of a near-synchronous orbit: density distribution in the GEO ring after 2 days, for fragments larger than 1 mm, 1 cm and 10 cm.

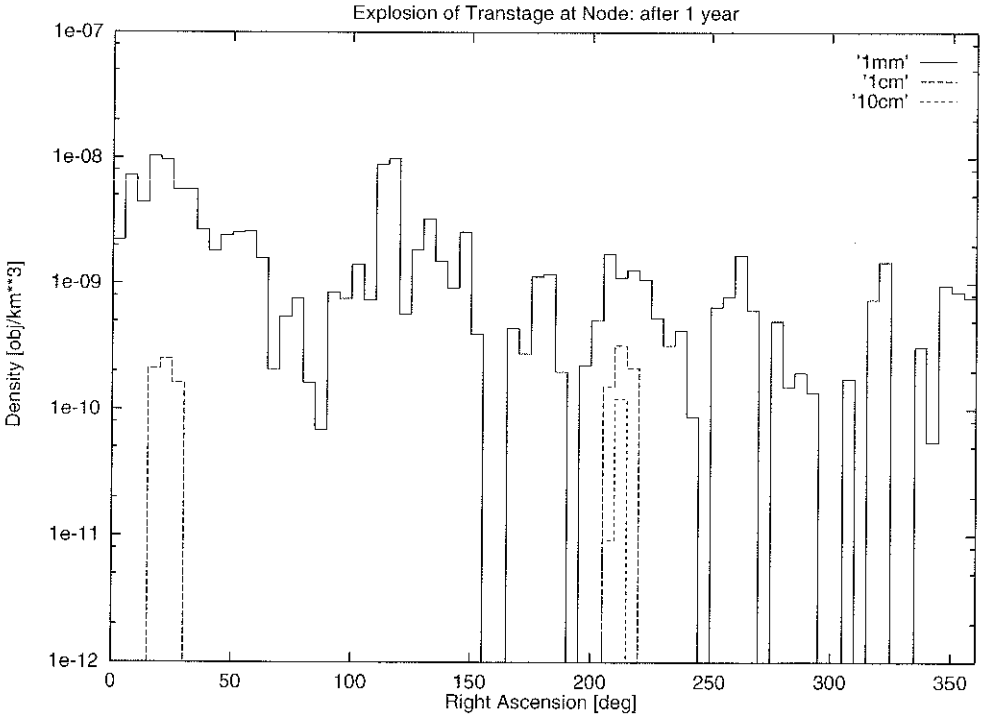

Fig. 10. Explosion at the ascending node of a near-synchronous orbit: density distribution in the GEO ring after 1 year, for fragments larger than 1 mm, 1 cm and 10 cm.

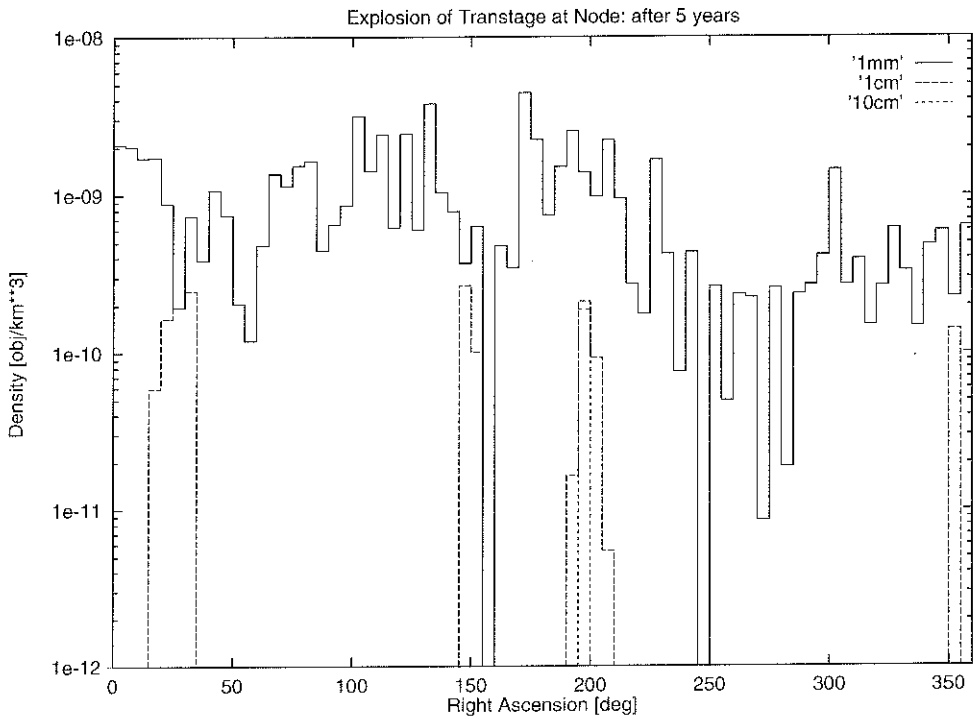

Fig. 11. Explosion at the ascending node of a near-synchronous orbit: density distribution in the GEO ring after 5 years, for fragments larger than 1 mm, 1 cm and 10 cm.

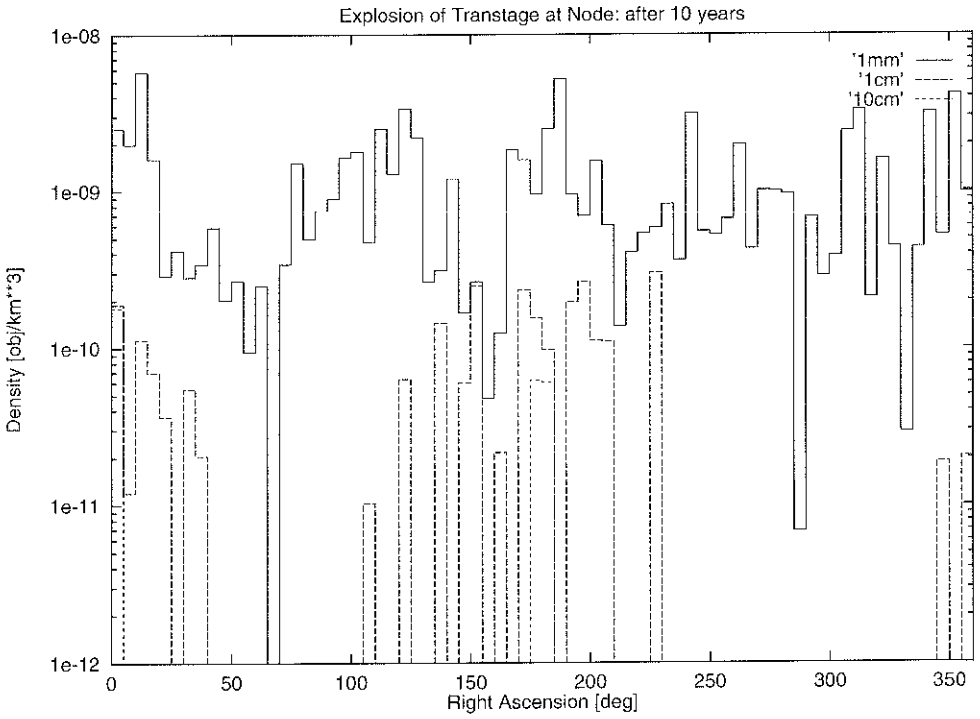

Fig. 12. Explosion at the ascending node of a near-synchronous orbit: density distribution in the GEO ring after 10 years, for fragments larger than 1 mm, 1 cm and 10 cm.

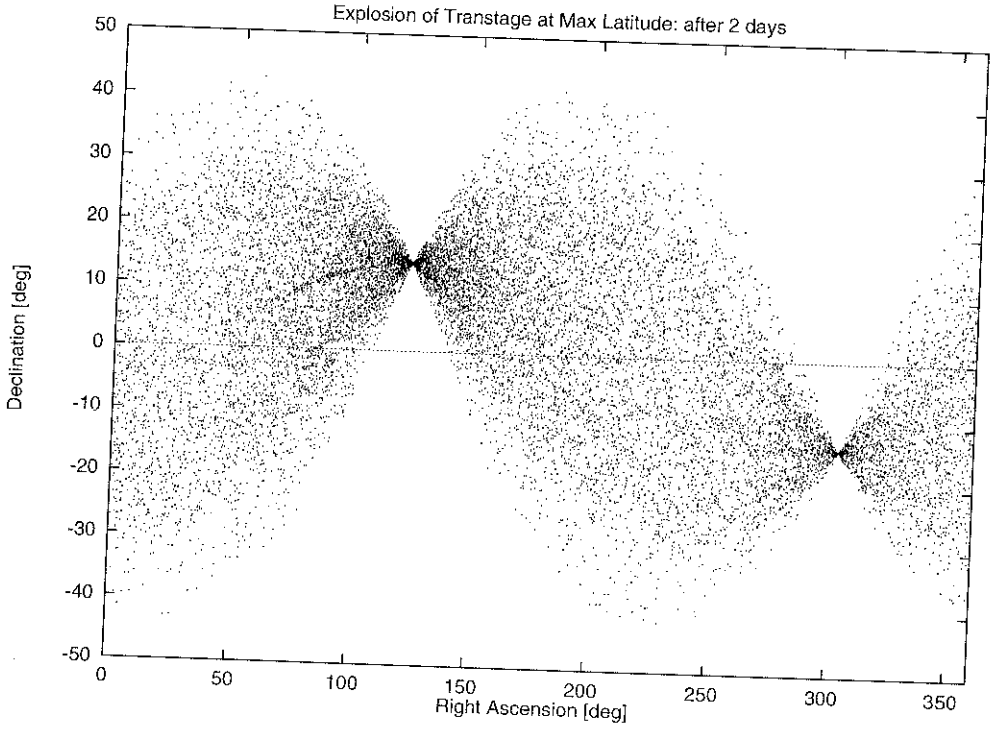

Fig. 13. Explosion at the maximum declination of a near-synchronous orbit: distribution of the fragments, in right ascension and declination, after 2 days.

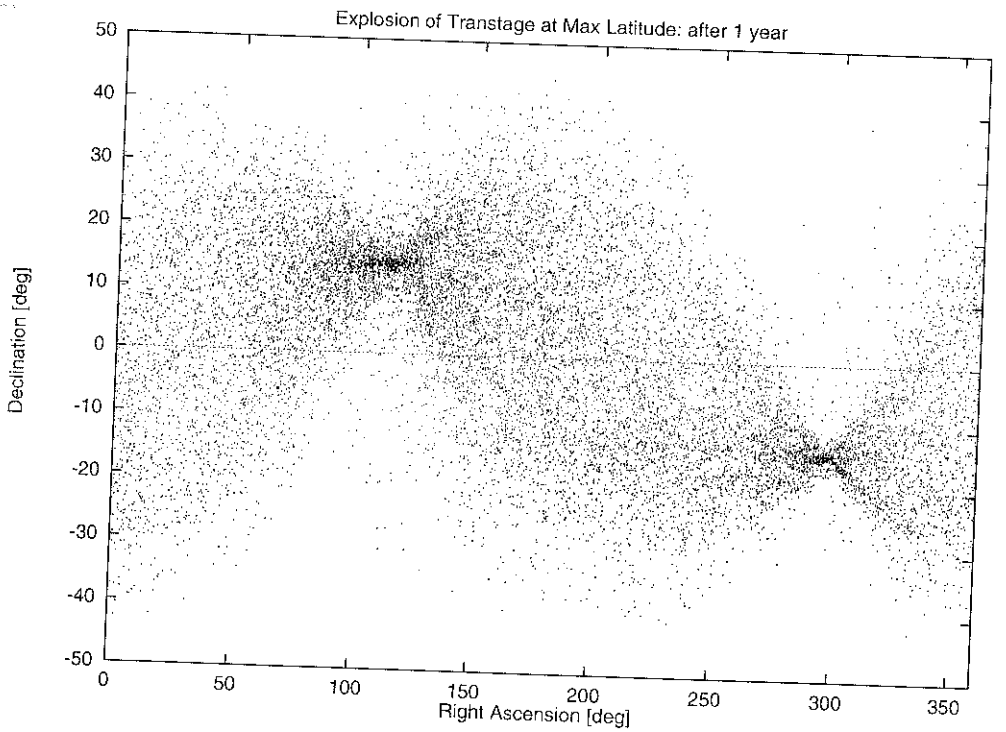

Fig. 14. Explosion at the maximum declination of a near-synchronous orbit: distribution of the fragments, in right ascension and declination, after 1 year.

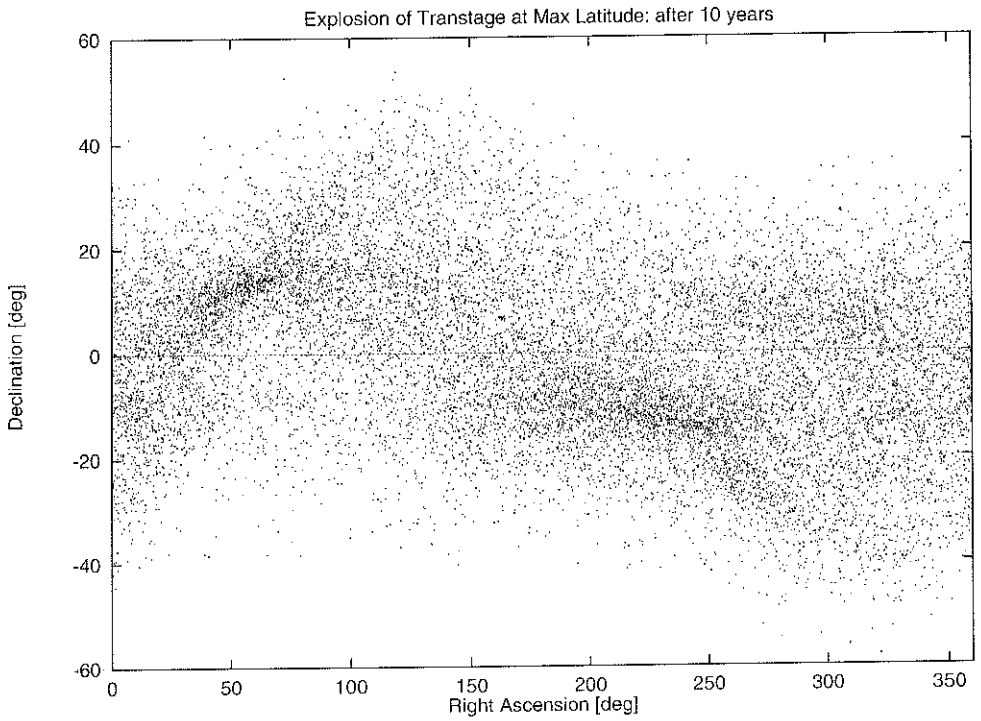

Fig. 15. Explosion at the maximum declination of a near-synchronous orbit: distribution of the fragments, in right ascension and declination, after 10 years.

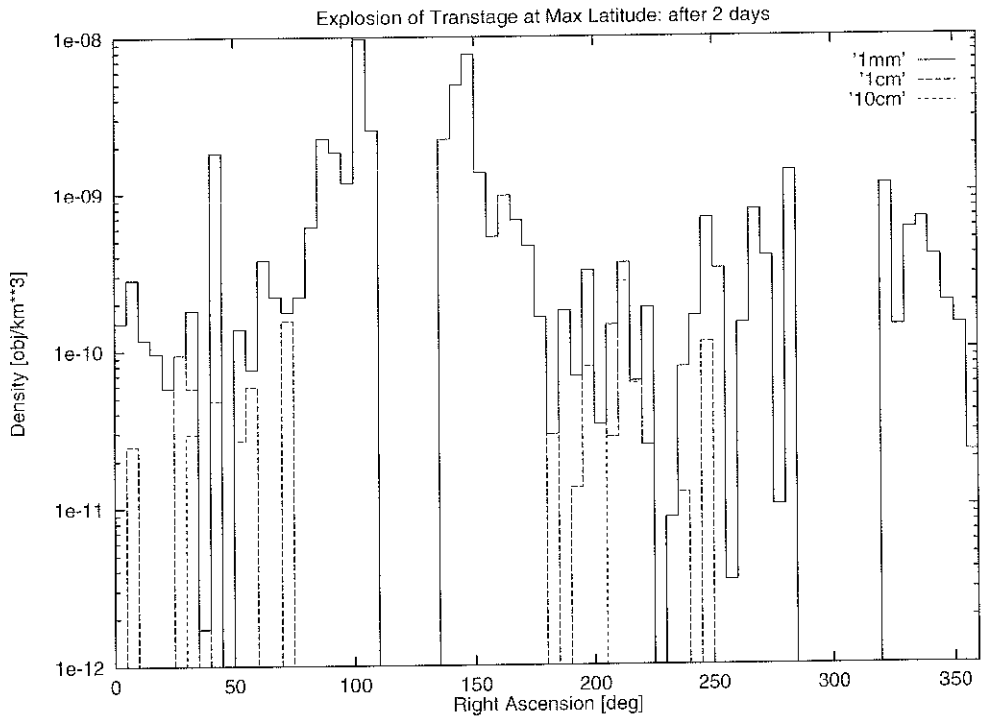

Fig. 16. Explosion at the maximum declination of a near-synchronous orbit: density distribution in the GEO ring after 2 days, for fragments larger than 1 mm, 1 cm and 10 cm.

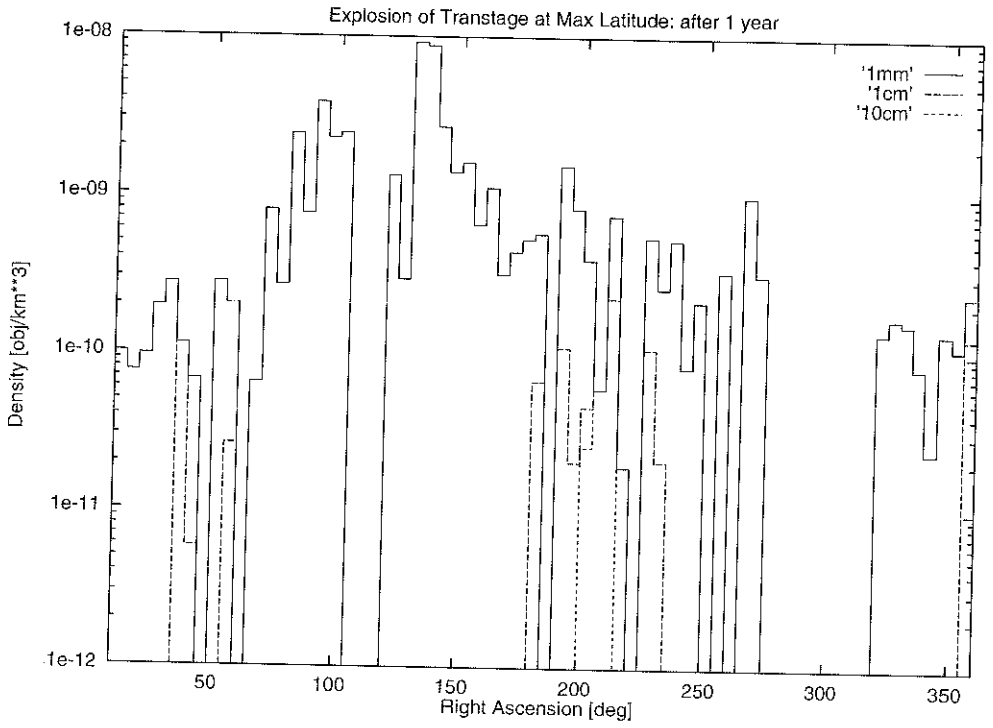

Fig. 17. Explosion at the maximum declination of a near-synchronous orbit: density distribution in the GEO ring after 1 year, for fragments larger than 1 mm, 1 cm and 10 cm.

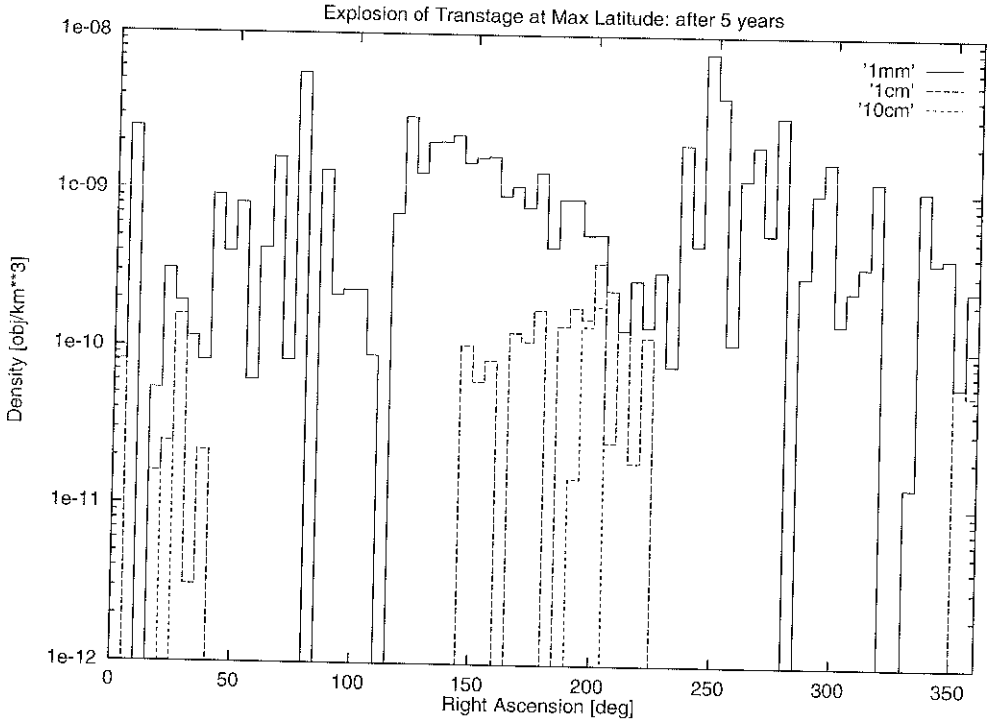

Fig. 18. Explosion at the maximum declination of a near-synchronous orbit: density distribution in the GEO ring after 5 years, for fragments larger than 1 mm, 1 cm and 10 cm.

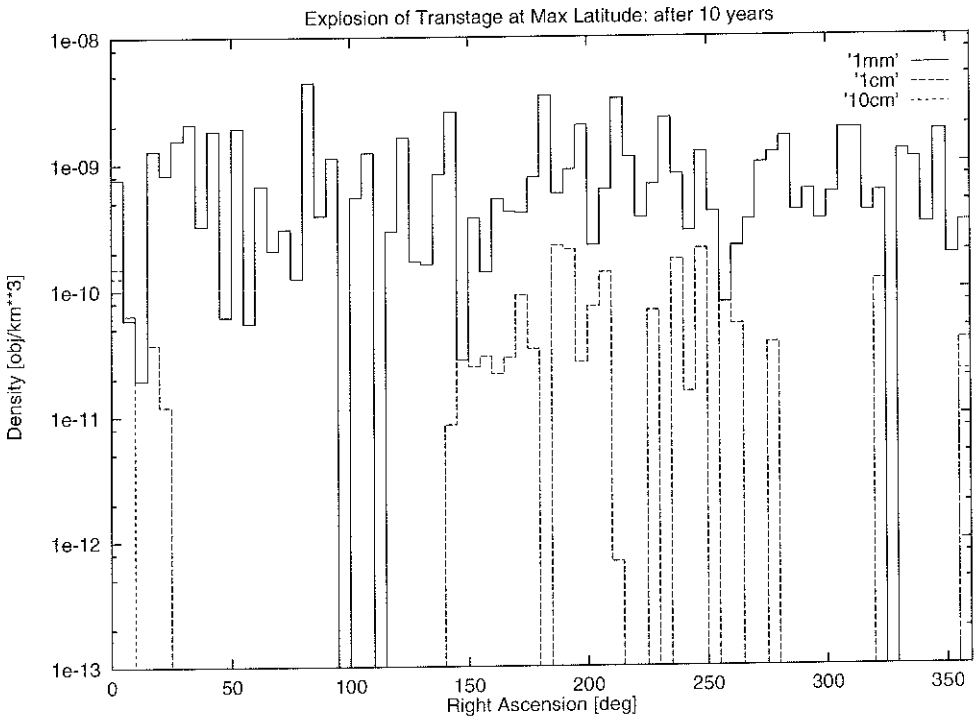

Fig. 19. Explosion at the maximum declination of a near-synchronous orbit: density distribution in the GEO ring after 10 years, for fragments larger than 1 mm, 1 cm and 10 cm.

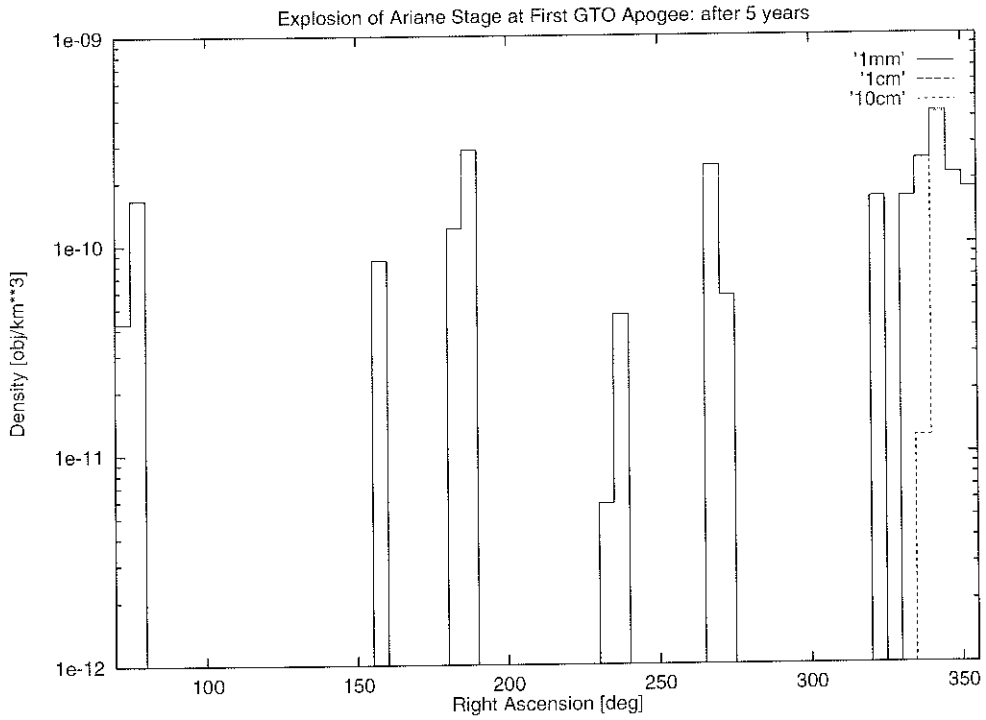

Fig. 20. Explosion at the first apogee of a GTO: density distribution in the GEO ring after 5 years, for fragments larger than 1 mm, 1 cm and 10 cm.

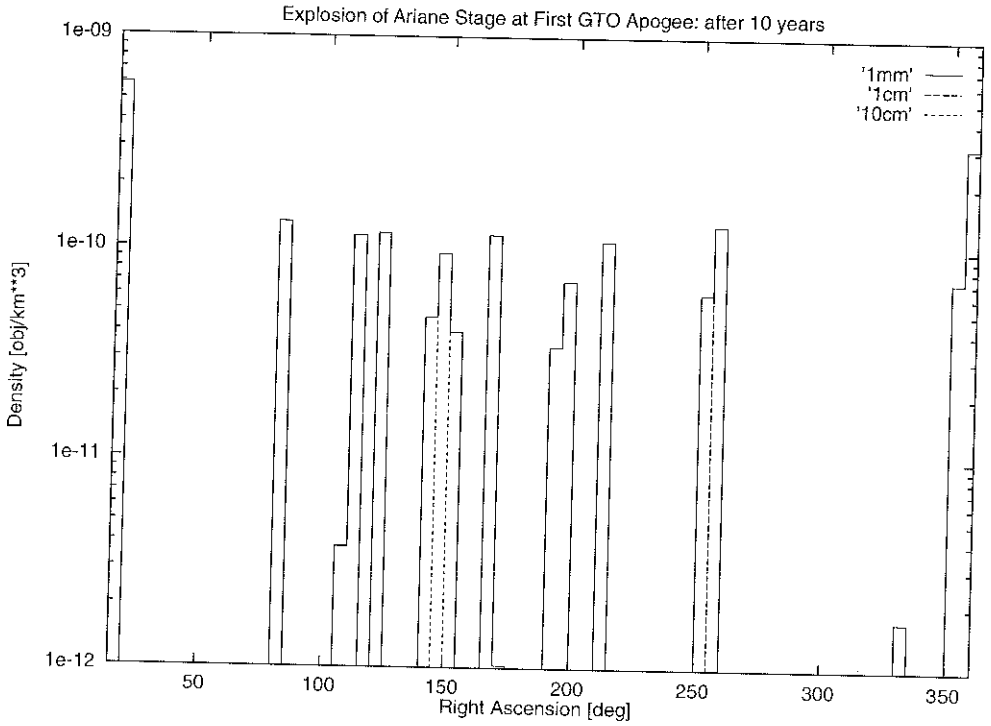

Fig. 21. Explosion at the first apogee of a GTO: density distribution in the GEO ring after 10 years, for fragments larger than 1 mm, 1 cm and 10 cm.

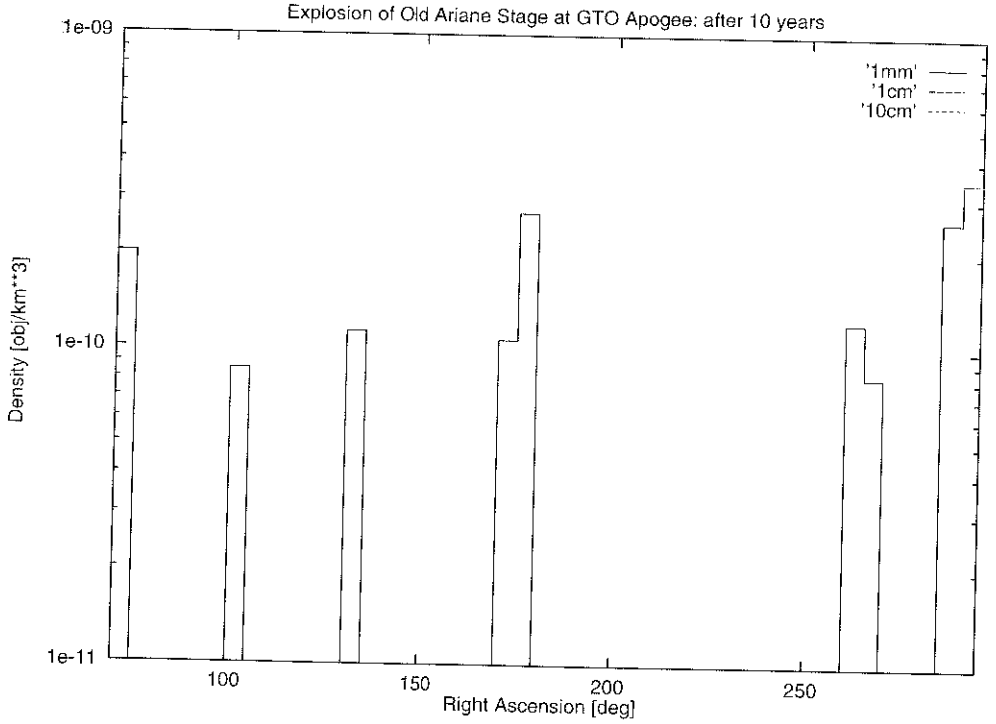

Fig. 22. Explosion at the apogee of a 4.5 months old GTO: density distribution in the GEO ring after 10 years, for fragments larger than 1 mm, 1 cm and 10 cm.